Transfection via whole-cell recording in vivo: Bridging single-cell physiology, genetics and connectomics

Ede A Rancz, Kevin M. Franks, Martin K. Schwarz, Bruno Pichler, Andreas T. Schaefer, Troy W Margrie

▶ **To cite this version:**

Ede A Rancz, Kevin M. Franks, Martin K. Schwarz, Bruno Pichler, Andreas T. Schaefer, et al.. Transfection via whole-cell recording in vivo: Bridging single-cell physiology, genetics and connectomics. Nature Neuroscience, 2011, 10.1038/nn.2765 . hal-00616226

HAL Id: hal-00616226
https://hal.science/hal-00616226

Submitted on 20 Aug 2011

HAL is a multi-disciplinary open access archive for the deposit and dissemination of scientific research documents, whether they are published or not. The documents may come from teaching and research institutions in France or abroad, or from public or private research centers.

L'archive ouverte pluridisciplinaire **HAL**, est destinée au dépôt et à la diffusion de documents scientifiques de niveau recherche, publiés ou non, émanant des établissements d'enseignement et de recherche français ou étrangers, des laboratoires publics ou privés.

Transfection via whole-cell recording *in vivo*: bridging single-cell physiology, genetics and connectomics

Rancz, Ede A.[1,2*], Franks, Kevin M. [1, 3*], Schwarz, Martin .K.[4], Pichler, Bruno[2], Schaefer, Andreas T.[1,5], and Margrie, Troy W.[1,2]

[1]Department of Neuroscience, Physiology and Pharmacology, University College London, Gower Street WC1E 6BT, London, UK. [2]Division of Neurophysiology, The National Institute for Medical Research, Mill Hill NW7 1AA, UK. [3]Department of Neuroscience, Columbia University, 701 W. 168th St, New York, NY 10032, USA. [4]Department of Molecular Neurobiology, Max Planck Institute for Medical Research, Jahnstrasse 29, 69120 Heidelberg, Germany. [5]SNWG Behavioural Neurophysiology, Max Planck Institute for Medical Research, Jahnstrasse 29, 69120 Heidelberg, Germany

[*] These authors contributed equally

Words in Abstract: 150
Total words in text: 5256 (excluding references)
Number of figures: 4

Corresponding author:
Professor Troy W. Margrie,
Division of Neurophysiology,
The National Institute for Medical Research,
Mill Hill NW7 1AA, UK.
Tel: +44 20 8816 2236;
e-mail: troy.margrie@nimr.mrc.ac.uk

Single cell genetic manipulation is expected to significantly advance the field of systems neuroscience. However, existing gene delivery techniques do not permit electrophysiological characterization of cells that would establish an experimental link between physiology and genetics for understanding neuronal function. Here we demonstrate in the mouse brain *in vivo* that (i) neurons remain intact after 'blind' whole-cell recording, (ii) that DNA vectors can be delivered through the patch-pipette during such recordings and (iii) that these vectors drive protein expression in recorded cells for at least seven days. We illustrate the utility of this approach by recording visually-evoked synaptic responses of primary visual cortical cells while delivering DNA plasmids that permit retrograde, mono-synaptic tracing of that neuron's presynaptic inputs. By providing a biophysical profile of the cell prior to its specific genetic perturbation, this combinatorial method has captured the first synaptic and anatomical receptive field of a neuron.

A central goal for neuroscience is to understand how neurons in the brain and spinal cord process information. Ultimately this requires obtaining information from combined electrophysiological, neuroanatomical, optical and genetic methods that together can address the necessary broad range of questions from the level of genes and molecules, up to single cells and circuits[1-9]. Electrical recording methods, such as the whole-cell patch-clamp technique, can provide a relatively complete biophysical characterization of an individual neuron. Its recent optimization for *in vivo* applications has afforded increased stability and longevity such that the intrinsic, synaptic and spiking properties of cells in many superficial[10-13], and deep structures[14-18] have been obtained. This method has been especially useful for

determining the synaptic receptive fields of single cells in anesthetized [14], awake head-fixed[14, 17, 19] and freely moving[20] preparations so that synaptic activity may be linked directly to sensory processing[16] and behavior[17, 18].

Concurrently, recent developments in optogenetics[8, 21, 22] and virus-based circuit tracing[3, 4, 23] are providing effective tools for manipulating and tracing neuronal circuits both *in vitro* and *in vivo*. For example, genetically controlling expression of channel- or halorhodopsin make it possible to selectively excite or inhibit the activity of defined sets of neurons *in vivo*[8, 24]. Viral strategies for expression are also becoming increasingly useful for spatially, temporally and genetically controlling network function[3, 25] and even tracing the anatomical connectivity of a single cell[26]. At present however, there is no method available that delivers both single cell electrophysiology and genetic manipulation. Application of such a tool could be used to provide answers to questions that are fundamental to our understanding of the role of single neurons within the context of a local network in the intact animal[27].

The relatively large tip size of patch pipettes not only permits low-resistance intracellular recordings but readily allows dialysis of exogenous materials into the recorded cell[12, 14, 28], which raises the possibility of delivering macromolecules such as plasmids. Here we examine the feasibility of combining *in vivo* whole-cell recording and gene delivery by answering four specific questions: Do cells survive for significant periods following whole-cell recording in vivo? What is the likelihood and longevity of whole-cell recordings with internal solutions containing plasmid DNA? Can plasmid DNA dialyze into the cell and drive protein expression? Is protein

expression restricted to only the patched cell?

After demonstrating the feasibility of this approach we then highlight its potential by recording the synaptic responses of neurons in mouse primary visual cortex to presentation of drifting gratings, while delivering vectors to permit monosynaptic retrograde labeling using a modified rabies virus[23]. Several days after virus injection we observed unprecedented numbers of labeled neurons permitting registration of a cell's synaptic receptive field and the presynaptic cells that define it.

RESULTS

(i) Recovery rates of *in vivo* whole-cell recorded neurons

It is generally assumed that whole-cell recording substantially compromises cell viability. Therefore, when morphological confirmation is required following *in vivo* whole-cell recording, animals are usually immediately sacrificed and the tissue fixed for histological analysis[29]. We first directly tested this assumption by performing *in vivo* whole-cell recordings from cells in layers 2-5 of mouse neocortex using a biocytin-containing intracellular solution and assessing the incidence and morphology of labeled neurons several days after recording. The method for obtaining whole-cell recordings was essentially as described previously[14]. Briefly, a glass electrode was filled with a potassium-based intracellular solution and advanced quickly to the target depth under moderate positive pressure (**Fig. 1a**). The positive pressure was then reduced and the electrode was advanced while the tip-resistance was monitored. The pressure was removed upon 'hitting' a cell, judged by changes in the tip-resistance (**Fig. 1b**), and negative pressure was applied to help seal formation

(**Fig. 1c**). Whole-cell access was achieved by brief bursts of negative pressure to rupture the cell membrane (**Fig. 1d**). In the whole-cell configuration and in current clamp mode, the current-voltage relationship (**Fig. 1e**) and spontaneous and evoked activity was recorded. At the end of the recording the patch pipette was slowly withdrawn while constantly monitoring the access resistance in voltage-clamp mode (**Fig. 1f**,**g**). Pipette retraction usually resulted in membrane resealing (**Fig. 1g**) and formation of an outside-out patch (**Fig. 1h**) that was considered an important, though not essential, predictor of cell viability. Following whole-cell recording, mice were recovered and returned to their home cages (see methods).

To assess the survival rate of recorded neurons, mice were sacrificed 24-51 hours after recording, the brain removed, fixed and slices were prepared (see methods). The vast majority of cells recorded were pyramidal cells and their recovered morphologies typically included the apical dendrite that extended up to layer 1 (**Fig. 1i**). The morphological criterion for identifying determining cells was that the cell soma and the proximal regions of at least four dendrites were visible. The number of recovered cells per brain that met this criterion never exceeded the number of cells recorded.

Our criteria for considering recorded cells as being potentially recoverable included that the initial series resistance was below 80 MΩ (**Fig. 1j**). In most cases (>90%), these recordings were actively terminated as described above (**Fig. 1**). In 10 cases where retraction criterion was not met or series resistance was above 80 MΩ, another recording in the same animal was successfully obtained at a different

cortical depth. In these cases we recovered 3/10 cells that did no satisfy both criteria (**Fig. 1j**, grey circles). Cells that do not meet our criteria have not been included in the recording duration and recovery interval analysis. Parameters such as recording duration (up to 13 minutes) and recovery interval (up to 51 hours) did not correlate with the likelihood of observing biocytin filled cells (**Fig. 1k**,**l**). According to these criteria, we recovered 78% (47/60) of recorded cells following biocytin visualization with Atto-565 or Alexa-488 conjugated streptavidin (**Fig. 1i**). This indicates that neurons can reliably survive whole-cell recording and maintain their structural integrity.

(ii) Whole-cell recordings with internal solutions containing plasmid DNA

To determine the feasibility of DNA loading during whole-cell recording we next performed recordings with intracellular solutions containing up to 350 ng/µl of plasmid DNA encoding fluorescent proteins (see methods) and biocytin. Qualitatively, we found that the likelihood of obtaining seals and low-resistance recordings with internal solutions containing DNA was similar to that using standard internals.

Cells recorded with plasmid DNA in the pipette had firing profiles typical of cortical neuronal subclasses[15, 29, 30] (**Fig. 2a**). Based on stable resting membrane potentials, ongoing synaptic activity (**Fig. 2b**) and overshooting action potentials (**Fig. 2b**), cells remained healthy for the duration of the recording (typically 5-13 minutes). All recordings were actively terminated after the intrinsic biophysical properties (**Fig. 2a**) and synaptic receptive fields of cells were obtained (**Fig. 2c**).

After slowly retracting the pipette, mice were allowed to recover for at least 24 hours (range 24-51 hours) before sacrificing. Usually only one cell was recorded per animal, though in some mice several cells (typically two) were recorded in different layers, allowing electrophysiology and GFP fluorescence to be unambiguously matched. All recordings for these experiments were actively and successfully terminated.

(iii) Protein expression

We found that we often recovered intensely fluorescent cells, which were always in the expected locations and had elaborate dendritic morphologies consistent with predictions from electrophysiological data (**Fig. 2a**,**b**). Of the 39 cells recorded with internal solution containing DNA, 22 were found to express GFP. In all cases where GFP labeled cells were observed (within 51 hours after recording), cells were also positive for biocytin (**Fig. 2d1**,**d2**). Nine cells were however found to be biocytin positive and did not express GFP. Following immuno-histochemical amplification, GFP-positive cells always showed label in dendritic spines and the axon (**Fig. 2e**). Unlike the biocytin label, we only observed expression of the fluorescent protein in single cells and never along the electrode tract (cf; **Fig 2d1**,**d2**). As with recordings with biocytin, we observed a similar effect of series resistance on recovery probability (**Fig. 2f**) while recording duration and recovery interval appeared to have no such impact (**Fig. 2g**,**h**). Thus, following whole-cell recording with plasmid-containing intracellular solution, 56% of cells expressed fluorescent protein specifically in, and only in the recorded cell.

There exist obvious advantages in delivering multiple genes into a specific neuron that has been electrophysiologically characterized. We therefore next enquired whether multiple vectors could be reliably co-expressed by including two or three types of plasmids encoding proteins fluorescent at different wavelengths (e.g. td-Tomato, Cerulean, Venus) in our intracellular solution. For experiments using multiple plasmids, 3/7 cells were recovered, and fluorescence was observed at all appropriate wavelengths in all recovered cells (**Fig. 3a**,**b**).

Together, these results show that neurons can survive *in vivo* whole-cell recordings. DNA plasmids in the intracellular solution do not impair electrophysiological characterization of cells but readily dialyze into the neuron resulting in expression of exogenous genes. Since plasmid DNA expelled into the extracellular space is not expressed, transfection is restricted to the recorded cell. This method therefore appears ideally suited to span neurophysiological and genetic approaches for understanding the function of specific cells and circuits *in vivo*.

Application: bridging single cell function and connectivity

A method describing monosynaptic control of modified rabies virus spread into presynaptic neurons has recently been reported[23]. It is widely accepted that the native, non-modified rabies virus infects synaptically connected neurons exclusively in the retrograde direction[31,32], a process that relies on the rabies virus glycoprotein (RV-G)[33,34]. When the RV-G gene is deleted and replaced by a fluorescent protein-encoding gene, this modified rabies virus is rendered incompetent for trans-synaptic

infection, but can replicate inside the initially infected cell. Infection by RV-G-deficient rabies virus encapsulated with the avian sarcoma and leucosis virus envelope protein (*SAD-ΔG-mCherry-EnvA*) is restricted to only those cells that express an avian receptor protein (TVA) that is not expressed in mammals. Thus, by transfecting a single cell with vectors expressing TVA and RV-G, only this cell will be (i) susceptible to initial infection (via TVA) and (ii) provides the incompetent virus with RV-G required for trans-synaptic infection. The virus can therefore spread from the primarily infected cell to its presynaptic inputs and express fluorescent protein in these cells. However, since RV-G is not expressed in the presynaptic cells, the virus can spread no further. This approach therefore labels only first-order neurons presynaptically connected to the primary cell[23, 26, 32].

To demonstrate the potential of genetic manipulation via whole-cell recording *in vivo* to bridge our understanding of cell function and connectivity we first recorded the intrinsic properties (**Fig. 4a**) and visually-evoked synaptic responses (**Fig. 4b**) of a layer 5 pyramidal cells in mouse visual cortex (n = 8) to drifting gratings of different orientations (see methods). Synaptic responses were more broadly tuned than spiking output but showed clearly similar orientation preferences[35, 36] (**Fig. 4b,c**). Furthermore, and in an orientation-specific manner, the evoked synaptic activity fluctuated substantially during such responses (**Fig. 4c**). During functional characterization we simultaneously delivered a vector that directed expression of both the TVA receptor and RV-G, and a second vector directing expression of GFP (**Fig. 4d**,**e**). Two days after recording we injected ~200nl of *SAD-ΔG-mCherry-EnvA* into layer 5.

Between four and thirteen days after injection animals were transcardially perfused, sacrificed (n = 8) and 100 or 200 µm thick brain slices were prepared (see methods). Fluorescent signals were then imaged using confocal microscopy[37]. In 3 of the 8 animals we observed hundreds of mCherry-expressing neurons (n = 152, 221, 666; **Fig. 4d**–**g**; Supplementary Fig. 1) within and outside primary visual cortex. In 2 of the remaining 5 mice we observed a single GFP-expressing cell but no mCherry signal, most likely indicating successful transfection in cells that were not subsequently infected with the pseudotyped rabies virus. In the remaining 3 mice we failed to detect cells expressing either GFP or mCherry. In control animals (n = 2) that only received virus injection (500 nl) we observed a total of 6 mCherry-positive glia and 1 neuron (Supplementary Fig. 1). These data show that by combining in vivo whole-cell transfection with trans-synaptic tracing methods it is possible to record the synaptic receptive fields of neurons while delivering the genetic machinery necessary to successfully identify the presynaptic cells that transmit such signals.

DISCUSSION

Here we have shown that the whole-cell patch clamp method can be used to transfect single cells during neuronal recording *in vivo*. Perhaps the most surprising aspect of the data presented here is the high survival rate after *in vivo* whole-cell recording. This finding is in line with a previous study where, in acute cortical slices neurons that are patched, and then re-patched up to 12 hours later, remain healthy though their connectivity may be altered[38]. Here, we have investigated cell mortality rates *in vivo* up to 51 hours post recording using morphological criteria. Consistent with data obtained from slices, the large number of healthy neurons observed after *in vivo* recording ensures that the likelihood of genetic manipulation is relatively high (~50 %). Following DNA delivery via whole-cell recording *in vivo*, cells remain viable since they continue to express reporter proteins for up to a week. During this time recorded cells are also able to withstand viral infection and its subsequent demands placed on their metabolic processes.

This is the first demonstration that DNA may be delivered into neurons via an intracellular recording method. This approach should therefore be considered useful for any experimental system including neuronal and non-neuronal cultures where cells can be maintained for extended periods of time. In combination with electrically recording from the cell, the list of potential applications of this method ranges from genetic perturbation of intracellular signaling cascades, up- or down-regulation of ion channels, membrane receptors, light-activatable ion channels or genetically encoded indicators, expressed across functionally-related presynaptic circuits.

Series resistance appears to be the most important factor influencing the recovery rate of both biocytin-filled and DNA loaded cells. Again, this is in line with previous reports indicating that the efficiency of loading substances such as dyes and biocytin is reduced as series resistance increases[28]. As with dye loading, the relatively low access resistance of intracellular recordings obtained with the patch pipettes used *in vivo* are suitable for DNA delivery. In cases where we recovered cells recorded with intracellular solutions containing multiple reporter plasmids, we always observed all of the expected fluorescent proteins (up to three). Though we have not established an upper limit, this suggests that our transfection approach results in the successful delivery of many plasmids. Given that plasmids may contain more that one protein-encoding sequence, a substantial number of genes may be simultaneously delivered via this method.

Here we used modified rabies virus-mediated monosynaptic retrograde tracing to demonstrate one application of combined whole-cell recording and multi-gene delivery. During recording of intrinsic properties and visually-evoked synaptic responses we delivered genes to direct infection and spread of *SAD-ΔG-mCherry-EnvA* in the recorded cell. The resulting number of mCherry-labeled cells presynaptic to layer 5 neurons shown here substantially exceeds that for Layer 2/3 cells observed in a recent electroporation study[26]. This disparity may reflect differences between the connectivity of layer 2/3 and layer 5 pyramidal neurons. However, the difference in the extent of presynaptic labeling may also reflect differences in the efficiency of plasmid delivery and protein expression between these two methods.

Genetic manipulations via electroporation has been complemented with two-photon imaging to allow targeted gene delivery to single neurons in the mouse brain,[26] with similar success rates to that reported here. Though such a targeted electroporation method is promising, its application is somewhat limited. Specifically, although action potentials in the target cell could, in principle, be detected[39] prior to electroporation, cell attached recordings are highly restricted since they preclude measurements of synaptic and intrinsic properties. Secondly, successful single-cell *in vivo* electroporation has required visualization[26, 40, 41], limiting this method to superficial cells in the intact brain. Although the whole-cell transfection method described here can certainly be combined with optical monitoring to target specific cell types[30, 41], we have used blind whole-cell recordings for single-cell transfection in optically inaccessible, deeper structures[14-18]. It therefore appears that any cell type that can be patched can be genetically modified in the process.

Wild-type rabies virus has long been used as an extremely reliable retrograde trans-neuronal tracer[32]. By combining whole-cell recording and DNA delivery, with retrograde tracing using modified rabies virus, we have determined both the physiological properties and connectivity profile of a single neuron. By further combining this with either bolus loading of calcium dyes[42] or using virus-mediated genetically driven expression of calcium indicators[43-45] it will be possible to implement *in vivo* two-photon based population imaging[2, 42, 46-48] (at least of cells in upper cortical layers) to investigate temporal correlations of firing of known presynaptic cells and the unique synaptic responses recorded from the postsynaptic

neuron. It will be interesting, for example, to investigate whether commonalities in connectivity reflect any bias in function.

Only by probing both the function and connectivity of specific cells and circuits can we obtain a complete understanding of the functional architecture of the brain[27]. The method of DNA delivery via whole-cell recording described here provides a versatile new tool for assaying and manipulating both single cells and probing the functional connectivity of specific local and long-range networks.

Acknowledgements

KMF thanks Steven Siegelbaum and Richard Axel for their generous support and encouragement, and Abigail Mulligan for technical assistance. We also thank Peter H. Seeburg for support and Diogo Castro, Ben Matynoga and Daniela Drechsel for advice. We thank Karl-Klaus Conzelmann for gifting rabies virus *SAD⊿G-mCherry* and Péter Boross, Ed Callaway, Hendrik Wildner and Francois Guillemot for helpful discussions and reagents. EAR is a Sir Henry Wellcome Postdoctoral Fellow. This work was supported by The Robert Leet and Clara Guthrie Patterson Trust and a NIDCD K99 grant (KMF), The Max-Planck Gesellschaft (ATS, MS), The MRC and The Alexander Von Humboldt Foundation (TWM).

Author Contributions

EAR, KMF, ATS, and TWM conceived experiments. KMF, ATS and TWM performed original proof-of-principle and multi-plasmid experiments. EAR collected the biocytin, GFP and viral tracing data. MKS co-designed and generated plasmids and provided virus. BP provided customized visual stimulation and compiled large-scale imaging data. EAR, KMF and TWM wrote the manuscript with input from all other authors.

Figure 1: Recording methodology and biocytin recovery rates

a, Seal test current trace used to monitor pipette resistance. **b,** Contact with cell membrane while stepping the electrode indicated by rhythmic changes in pipette resistance associate with heartbeat-related movement. **c,** Traces showing seal formation and **d,** whole-cell access. **e,** IV relationship (current injections 50 pA steps for 600 ms) recorded from the cell shown in i. **f,** Current traces in response to voltage steps immediately prior and **g,** during pipette retraction whereby the outside-out patch configuration is achieved **h**. Inset trace: detail from **h** showing single channel currents. **i**, Example morphology of a biocytin-labeled layer 2/3 pyramidal cell (animal sacrificed 29 hours after recording). **j,** Success rates of biocytin-filled cell recovery plotted against series resistance of recording (determined within 30 seconds after break-in). Circles represent, on a cell-by-cell basis, recovery success or failure. Grey-filled circles indicate those recordings that did not meet retraction and/or series resistance criteria. Large open red circles represent the mean success for each bin (range: 20–40, 41–50, 53–70, 71–200 MΩ). All error bars are SD. Numbers indicate the n for the respective bin. Dashed lines are linear fits to the individual data points. **k,** Success rates of cell recovery plotted against duration of recording (bin ranges: 1–4, 5–6, 7–9 and 10–13 mins) and **l**, the interval between recording and sacrificing the animal (bin ranges: 23–24, 25–29, 31–45, 47–51 hours).

Figure 2: Physiological characterization and genetic manipulation

a, The firing profile and IV relationship recorded from the layer 5 neuron shown in panels d1 and d2. Voltage traces shown are in response to 50 pA current steps of 600 ms duration. **b,** Membrane voltage traces showing spontaneous synaptic activity and the kinetics of a resultant action potential. **c1,** Synaptic responses (average of 10 sweeps) to drifting gratings moving in the direction indicated by the arrows (left). Arrow (top) indicates onset of grating drift. **c2,** Polar plot showing integral of the membrane voltage traces (for 1400ms from stimulus onset). **d,** Layer 5 pyramidal cell in primary visual cortex 26 hours after recording showing GFP expression (**d1**) and biocytin-labeling (**d2**). Note the weak, non-specific biocytin signal along the electrode track due to the plume of biocytin expelled while approaching the recorded cell. **e**, GFP signal in dendritic spines and axonal arborizations in the same cell. **f,** Success rates of GFP-labeled cell recovery plotted against series resistance of recording (determined within 30 seconds after break-in). Circles represent, on a cell-by-cell basis, recovery success or failure. Grey-filled circles are cases that did not meet retraction and/or series resistance criteria. Open green circles represent the mean success for each bin (range 20–40, 41–50, 53–70, 71–200 MΩ. All error bars are SD. Numbers indicate the n for the respective bin. Dashed lines are linear fits to the individual data points. **g,** Success rates of cell recovery plotted against duration of recording (bin ranges: 1–4, 5–6, 7–8, 9–13 mins) and **h**, the interval between recording and sacrificing the animal (bin ranges: 23–25, 26–28, 29–33, 40–47, 48–51 hours).

Figure 3: Multiple gene delivery

a, Native fluorescence images of a layer 5 neuron patched in motor cortex 3 days after patching with *pCAGGS-tdTomato* (top right) and *pCAGGS-Cerulean* (50 ng/µl each bottom right), scale bar: 1 mm and 20 µm. **b**, Gallery of native fluorescence images for a layer 5 cell in primary somatosensory cortex 5 days after recording with *pCAGGS-DsRed2*, *pCAGGS-Venus* and *pCAGGS-ChR2-Cerulean*. Scale bar: 20 µm.

Figure 4: Synaptic receptive mapping and connectivity of a visual cortical neuron

a, The firing profile and IV relationship recorded from the GFP-expressing cell shown in panel d. Voltage traces shown are in response to 50 pA current steps of 600 ms duration. **b,** Synaptic responses (average of 10 sweeps) to drifting gratings moving in the direction indicated by the arrows (left). Arrow (top) indicates onset of drift. Current injection (–200 pA) was delivered to isolate evoked synaptic responses from AP activity. **c,** Polar plot showing integral of the voltage traces (red) recorded during the duration of the drifting grating. The integral of synaptic responses (1400 ms from stim onset) are normalized to largest response. Below are 5 example traces recorded for the least and most preferred orientation. For the spiking receptive field, holding current was removed and the stimulus sequence (b) was repeated five times. **d,** Coronal slice (100 µm thick) showing anti-GFP (green) and anti-RFP (red) fluorescence. The recorded layer 5 neuron (green-yellow) in primary visual cortex (V1) and mCherry-labeled cells (red) are clearly identifiable. In this slice approximately 200 presynaptic cells were observed. Scale bar = 500 µm. Abbreviations: V2ML: secondary visual cortex mediolateral, V2L: secondary visual cortex lateral, CA1–3: hippocampus fields CA1–3, DLG: dorsolateral geniculate nucleus. **e,** High magnification image showing GFP and mCherry labeled cells in V1. Scale bar = 100 µm. **f.** In this slice 8 mCerry-labeled cells were observed in the DLG. Scale bar = 50 µm. **g**. Five maximum intensity projections for consecutive 100 µm thick slices. The middle panel contains the host cell (green; scale bar: 200 µm). This mouse was sacrificed 7 and 9 days after virus injection and recording respectively.

References

1. Kleinfeld, D. & Griesbeck, O. From art to engineering? The rise of in vivo mammalian electrophysiology via genetically targeted labeling and nonlinear imaging. *PLoS Biol* 3, e355 (2005).
2. Helmchen, F. & Denk, W. Deep tissue two-photon microscopy. *Nat Methods* 2, 932-940 (2005).
3. Luo, L., Callaway, E.M. & Svoboda, K. Genetic dissection of neural circuits. *Neuron* 57, 634-660 (2008).
4. Arenkiel, B.R. & Ehlers, M.D. Molecular genetics and imaging technologies for circuit-based neuroanatomy. *Nature* 461, 900-907 (2009).
5. Geschwind, D.H. & Konopka, G. Neuroscience in the era of functional genomics and systems biology. *Nature* 461, 908-915 (2009).
6. O'Connor, D.H., Huber, D. & Svoboda, K. Reverse engineering the mouse brain. *Nature* 461, 923-929 (2009).
7. Scanziani, M. & Hausser, M. Electrophysiology in the age of light. *Nature* 461, 930-939 (2009).
8. Gradinaru, V.*, et al.* Molecular and cellular approaches for diversifying and extending optogenetics. *Cell* 141, 154-165 (2010).
9. Lichtman, J.W., Livet, J. & Sanes, J.R. A technicolour approach to the connectome. *Nature Reviews. Neuroscience* 9, 417-422 (2008).
10. Margrie, T.W., Sakmann, B. & Urban, N.N. Action potential propagation in mitral cell lateral dendrites is decremental and controls recurrent and lateral inhibition in the mammalian olfactory bulb. *Proceedings of the National Academy of Science, USA.* 98, 319-324 (2001).
11. Wehr, M. & Zador, A.M. Balanced inhibition underlies tuning and sharpens spike timing in auditory cortex. *Nature* 426, 442-446 (2003).
12. Waters, J., Larkum, M., Sakmann, B. & Helmchen, F. Supralinear Ca2+ influx into dendritic tufts of layer 2/3 neocortical pyramidal neurons in vitro and in vivo. *J Neurosci* 23, 8558-8567 (2003).
13. Loewenstein, Y.*, et al.* Bistability of cerebellar Purkinje cells modulated by sensory stimulation. *Nat Neurosci* 8, 202-211 (2005).
14. Margrie, T.W., Brecht, M. & Sakmann, B. In vivo whole-cell recordings from neurons in the anaesthetized and awake mammalian brain. *Pflügers Archive - European Journal of Physiology* 444, 491-498 (2002).
15. Brecht, M., Schneider, M., Sakmann, B. & Margrie, T.W. Whisker movements evoked by stimulation of single pyramidal cells in rat motor cortex. *Nature* 427, 704-710 (2004).
16. Arenz, A., Silver, R.A., Schaefer, A.T. & Margrie, T.W. The contribution of single synapses to sensory representation in vivo. *Science* 321, 977-980 (2008).
17. Harvey, C.D., Collman, F., Dombeck, D.A. & Tank, D.W. Intracellular dynamics of hippocampal place cells during virtual navigation. *Nature* 461, 941-946 (2009).
18. Epsztein, J., Lee, A.K., Chorev, E. & Brecht, M. Impact of spikelets on hippocampal CA1 pyramidal cell activity during spatial exploration. *Science* 327, 474-477.
19. Hromadka, T., Deweese, M.R. & Zador, A.M. Sparse representation of sounds in the unanesthetized auditory cortex. *PLoS Biol* 6, e16 (2008).

20. Lee, A.K., Epsztein, J. & Brecht, M. Head-anchored whole-cell recordings in freely moving rats. *Nat Protoc* 4, 385-392 (2009).
21. Zhang, F., Aravanis, A.M., Adamantidis, A., de Lecea, L. & Deisseroth, K. Circuit-breakers: optical technologies for probing neural signals and systems. *Nat Rev Neurosci* 8, 577-581 (2007).
22. Zhang, F., Wang, L.-P., Boyden, E.S. & Deisseroth, K. Channelrhodopsin-2 and optical control of excitable cells. *Nature Methods* 3, 785-792 (2006).
23. Wickersham, I.R.*, et al.* Monosynaptic restriction of transsynaptic tracing from single, genetically targeted neurons. *Neuron* 53, 639-647 (2007).
24. Huber, D.*, et al.* Sparse optical microstimulation in barrel cortex drives learned behaviour in freely moving mice. *Nature* 451, 61-64 (2008).
25. Komai, S.*, et al.* Postsynaptic excitability is necessary for strengthening of cortical sensory responses during experience-dependent development. *Nat Neurosci* 9, 1125-1133 (2006).
26. Marshel, J.H., Mori, T., Nielsen, K.J. & Callaway, E.M. Targeting single neuronal networks for gene expression and cell labeling in vivo. *Neuron* 67, 562-574 (2010).
27. Douglas, R.J. & Martin, K.A. Mapping the matrix: the ways of neocortex. *Neuron* 56, 226-238 (2007).
28. Eilers, J.K., A. A Practical Guide: Dye Loading with Patch Pipettes. in *Imaging in Neuroscience and Development* (ed. R.K. Yuste, A.) 277-281 (Cold Spring Harbour Laboratory Press, Cold Spring Harbour, New York, 2005).
29. Brecht, M.*, et al.* Organization of rat vibrissa motor cortex and adjacent areas according to cytoarchitectonics, microstimulation, and intracellular stimulation of identified cells. *J Comp Neurol* 479, 360-373 (2004).
30. Margrie, T.W.*, et al.* Targeted whole-cell recordings in the mammalian brain in vivo. *Neuron* 39, 911-918 (2003).
31. Ugolini, G. Specificity of rabies virus as a transneuronal tracer of motor networks: transfer from hypoglossal motoneurons to connected second-order and higher order central nervous system cell groups. *J Comp Neurol* 356, 457-480 (1995).
32. Ugolini, G. Advances in viral transneuronal tracing. *J Neurosci Methods*.
33. Mebatsion, T., Konig, M. & Conzelmann, K.K. Budding of rabies virus particles in the absence of the spike glycoprotein. *Cell* 84, 941-951 (1996).
34. Mebatsion, T. Extensive attenuation of rabies virus by simultaneously modifying the dynein light chain binding site in the P protein and replacing Arg333 in the G protein. *J Virol* 75, 11496-11502 (2001).
35. Ferster, D. Origin of orientation-selective EPSPs in simple cells of cat visual cortex. *J Neurosci* 7, 1780-1791 (1987).
36. Marino, J.*, et al.* Invariant computations in local cortical networks with balanced excitation and inhibition. *Nat Neurosci* 8, 194-201 (2005).
37. Conchello, J.-A. & Lichtman, J.W. Optical sectioning microscopy. *Nature Methods* 2, 920-931 (2005).
38. Le Be, J.V. & Markram, H. Spontaneous and evoked synaptic rewiring in the neonatal neocortex. *Proc Natl Acad Sci U S A* 103, 13214-13219 (2006).

39. de Kock, C.P. & Sakmann, B. Spiking in primary somatosensory cortex during natural whisking in awake head-restrained rats is cell-type specific. *Proc Natl Acad Sci U S A* 106, 16446-16450 (2009).
40. Nevian, T. & Helmchen, F. Calcium indicator loading of neurons using single-cell electroporation. *Pflugers Arch* 454, 675-688 (2007).
41. Kitamura, K., Judkewitz, B., Kano, M., Denk, W. & Hausser, M. Targeted patch-clamp recordings and single-cell electroporation of unlabeled neurons in vivo. *Nat Methods* 5, 61-67 (2008).
42. Stosiek, C., Garaschuk, O., Holthoff, K. & Konnerth, A. In vivo two-photon calcium imaging of neuronal networks. *Proc Natl Acad Sci U S A* 100, 7319-7324 (2003).
43. Tian, L.*, et al.* Imaging neural activity in worms, flies and mice with improved GCaMP calcium indicators. *Nat Methods* 6, 875-881 (2009).
44. Mank, M.*, et al.* A genetically encoded calcium indicator for chronic in vivo two-photon imaging. *Nature Methods* 5, 805-811 (2008).
45. Lutcke, H.*, et al.* Optical recording of neuronal activity with a genetically-encoded calcium indicator in anesthetized and freely moving mice. *Front Neural Circuits* 4, 9.
46. Ohki, K., Chung, S., Ch'ng, Y.H., Kara, P. & Reid, R.C. Functional imaging with cellular resolution reveals precise micro-architecture in visual cortex. *Nature* 433, 597-603 (2005).
47. Mrsic-Flogel, T.D.*, et al.* Homeostatic regulation of eye-specific responses in visual cortex during ocular dominance plasticity. *Neuron* 54, 961-972 (2007).
48. Rochefort, N.L.*, et al.* Sparsification of neuronal activity in the visual cortex at eye-opening. *Proceedings of the National Academy of Sciences* 106, 15049-15054 (2009).
49. Kugler, S., Kilic, E. & Bahr, M. Human synapsin 1 gene promoter confers highly neuron-specific long-term transgene expression from an adenoviral vector in the adult rat brain depending on the transduced area. *Gene Ther* 10, 337-347 (2003).
50. Brainard, D.H. The Psychophysics Toolbox. *Spat Vis* 10, 433-436 (1997).
51. Cetin, A., Komai, S., Eliava, M., Seeburg, P.H. & Osten, P. Stereotaxic gene delivery in the rodent brain. *Nat Protoc* 1, 3166-3173 (2006).

METHODS

Intracellular solutions

Intracellular solutions for whole cell recordings were made up in concentrated stock (1.2-3 times the final concentration) to allow for plasmid addition. The final concentrations were (in mM, all from Sigma-Aldrich or VWR International, UK.) 130 K-methanesulphonate, 10 Hepes, 7 KCl, 0.05 EGTA, 2 Na_2ATP, 2 MgATP, 0.5 Na_2GTP; pH was adjusted to 7.28 using KOH. The final osmolarity after adding either 0.5% biocytin or suspended plasmids was adjusted to the range of 280-290 mOsm. Intracellular solutions were filtered through a 0.2 µm pore size syringe filter (Whatman) or a 0.22 µm pore size centrifuge filter (Costar Spin-X). Spectrophotometry (NanoDrop 1000, Thermo Scientific) showed that DNA was not lost during filtration.

Plasmid production

The coding sequences of DsRed2, tdTomato, Venus, Cerulean or ChR2-Cerulean were subcloned into *pCAGG*s. For GFP we used *pCA-b-GFPm5 silencer 3* (generous gift from Hendrik Wildner and Francios Guillemot). For rabies virus mediated transneuronal tracing, coding sequences of rabies SAD-ΔG and TVA800[23] were linked with an internal ribosomal entry site (IRES2. DB Biosciences) and sub-cloned into *pCA-b-GFPm5 silencer 3* by replacing the GFP coding sequence. Correct insertion and coding sequences were verified by subsequent DNA sequencing. Resulting plasmids were transformed and individual clones were grown in E.coli Stbl3 (Invitrogen) cells to avoid recombination. DNA for *in vivo* recordings was prepared using an

endotoxin-free maxiprep kit (Qiagen) and suspended in ultrapure H_2O or TE buffer (Qiagen). Plasmid aliquots (10 µl) were diluted in H_2O and added to the intracellular solution for a final concentration of ~ 50–350 ng/µl.

Production of pseudotyped rabies virus

BHK cells were plated at a density of ~1.5 x 10^7. The following day, cells were transfected with 15 µg plasmid *pCAGG/SADΔG* (generous gift from Dr. Karl-Klaus Conzelmann) by CaP transfection. 24 h later rabies virus *SADΔG-mCherry* was added at a MOI of 3. 48 h later the *SADΔG-mCherry* containing supernatant was equally distributed onto four 15cm plates containing *pCAGGs/SAD-G* (15 µg/plate) transfected BHK cells (~1.5 x 10^7 cells/plate). Two days later the virus containing supernatant was applied onto four 15cm plates containing BHK-EnvARGCD cells [23] (~1.5 x 10^7 cells/plate) at a MOI of 1.5 for pseudotyping. 12 hours later cells were trypsinized and replated onto eight 15cm dishes. Pseudotyped rabies virus-containing supernatant was harvested 2 days later. The supernatant was spun at 2000 rpm at 4°C for 10 min. and subsequently filtered through a 0.45 µm filter. The filtered virus suspension was centrifuged for 90 min at 25000 rpm (SW28, 4 °C) in a Beckmann 80K ultracentrifuge. After centrifugation the supernatant was discarded and the pellet was aspirated in PBS. Pseudotyped rabies virus-containing solution was aliquoted in 10 µl aliquots and frozen at –70 °C. Virus titers were determined by serial dilution and over night infection of primary cortical neurons that had been infected with rAAV1/2 expressing *TVA800-IRES-GFP*[23] under control of the human synapsin promoter/ enhancer[49]. Three days later the number of red fluorescent, *SADΔG-mCherry* containing neurons were counted. Biological titers on TVA-

expressing neurons for *SADΔG-mCherry* for *in vivo* injections were ~2.5 x 10^7 /ml.

Surgical procedures

Young adult C57/BL6 mice (4–6 weeks old) were anaesthetized with a mixture of ketamine and xylazine (100 mg/kg and 10 mg/kg, respectively) injected intraperitoneally, supplemented as necessary whenever the animal showed toe-pinch reflexes. Mice were head-fixed using non-puncture ear-bars and a nose-clamp (SG-4N, Narishige, Japan), and their body-temperature maintained at 36–37 °C using a rectal probe and a heating blanket (FHC, Bowdoinham, ME, USA). An incision was made in the scalp and a small craniotomy was drilled above the relevant area of cortex using a dental drill (Osada Electric Co, Japan) and the dura removed. The surface of the brain was kept moist by applying sterile phosphate buffered saline solution (PBS, Sigma Aldrich) at regular intervals. Following recordings, the craniotomy was sealed using a silicone sealant (Kwik-Sil, World Precision Instruments) and the scalp sutured. The wound was infiltrated with lidocaine and a topical antibiotic (Cicatrin, GlaxoSmithKline, UK) was applied. The time from the initial anaesthesia to completing this procedure was kept as short as possible (< 2 hours). During recovery, mice were kept warm in a heating box (Harvard Apparatus, Holliston, MA, USA) for 3–4 hours under constant observation. All procedures were approved by the local ethics panel and UK Home Office under the Animals (Scientific Procedures) Act 1986.

Obtaining whole-cell recording

In vivo whole-cell recordings were carried out as described previously[14]. Briefly, glass

electrodes were pulled from borosilicate glass (GC150F, Harvard Apparatus Ltd, UK) on a vertical puller (PC-10, Narishige, Japan) to a tip resistance of 6–7 MΩ. Recordings were carried out with an AxoClamp 2B or Mulitclamp 700B amplifier (Axon Instruments, USA). Data were filtered at 3 KHz and digitized at 10–20 kHz using an ITC-18 A/D-D/A interface (InstruTECH, Heka Elektronik, Germany) and the Neuromatic package (www.neuromatic.thinkrandom.com) under Igor Pro 5 (www.wavemetrics.com).

Discontinuation of whole-cell recording

After a 2–16 minute recording, the patch pipette was slowly withdrawn (~3 μm/sec) while the seal test pulse was monitored in voltage clamp mode to determine access resistance. Often this resulted in pulling an outside-out patch of membrane, which we consider to be an important though not an essential criterion for cell survival. The electrical access to the cell could also be monitored by shifts in holding current due to ongoing synaptic input and in some cases the occurrence of unclamped action-currents. Applying a quick negative pressure pulse to abruptly break the seal with no indication of action currents indicated successful outside-out patch formation.

Synaptic receptive field mapping

Visual stimuli were generated using Matlab (Mathworks) and Psychophysics Toolbox[50]. Stimuli were presented on a 17 inch LCD monitor positioned 21 cm from the contralateral eye spanning 65° (vertical) and 81° (horizontal) of visual space. Stimuli consisted of 100 % contrast square wave gratings (spatial frequency 0.04

cycles/°) drifting in one of eight directions at 2.6 cycles/second. For each trial, one direction was chosen randomly and presented in the following sequence: stationary (1 second) - moving (1 second) - stationary (1 second).

Virus injections

For injections, long-shanked, volume-calibrated pipettes (Blaubrand) were pulled to achieve a tip size of approximately 10 µm diameter and tip-filled using negative pressure[51]. Animals were anesthetized as described above, sutures were removed and the Kwik-Sil covering the craniotomy was withdrawn. Injection pipettes were lowered as accurately as possible using the blood vessel pattern and under visual guidance along the same trajectory as recording pipettes to within 100–200 µm of the patched cell. Approximately 150–200 nl of virus solution was injected under 50 mbar of positive pressure for 2–3 minutes. The pipette was withdrawn, Kwik-Sil re-applied and the animal sutured and recovered.

Tissue processing and imaging

Brains were analyzed 1–9 days after recording. Deeply anaesthetised mice were usually transcardially perfused with cold PBS (0.1 M) followed by 4% paraformaldehyde (PFA) in PBS (0.1 M), though sometimes directly decapitated, and the brain was fixed in 4% PFA at 4 °C overnight. Coronal brain sections (100–200 µm) were cut on a vibrating microtome (Leica VT1200S or Microm HM 650V) and rinsed in PBS. Fluorescence images were acquired on a Leica SP1, SP5 or a Zeiss 510 laser-scanning confocal microscope. For experiments containing biocytin in the intracellular solution, slices were first treated with 1% Triton-X100 in PBS for 12

hours then incubated in a PBS solution containing either Atto-565- or Alexa-488-conjugated streptavidin (Sigma-Aldrich 1:100–1:200), 5% normal goat serum and 0.1% Triton-X for 12 hours at 4˚C. For immunostaining for GFP and mCherry, rabbit anti-GFP (Invitrogen 1:1000) and rat anti-RFP primary antibodies (Chromotek 1:1000; 24–48 hours at 4 °C) were visualized with donkey Alexa-488 anti-rabbit (Invitrogen 1:500) and goat Alexa-568 anti-rat (Invitrogen 1:500, 24 hours at 4 °C) secondary antibodies. After thorough washing in PBS, slices were mounted with an antifading medium (Mowiol 4-88, Calbiochem + 2.5% DABCO 33-LV, Sigma-Aldrich) and imaged as described above.

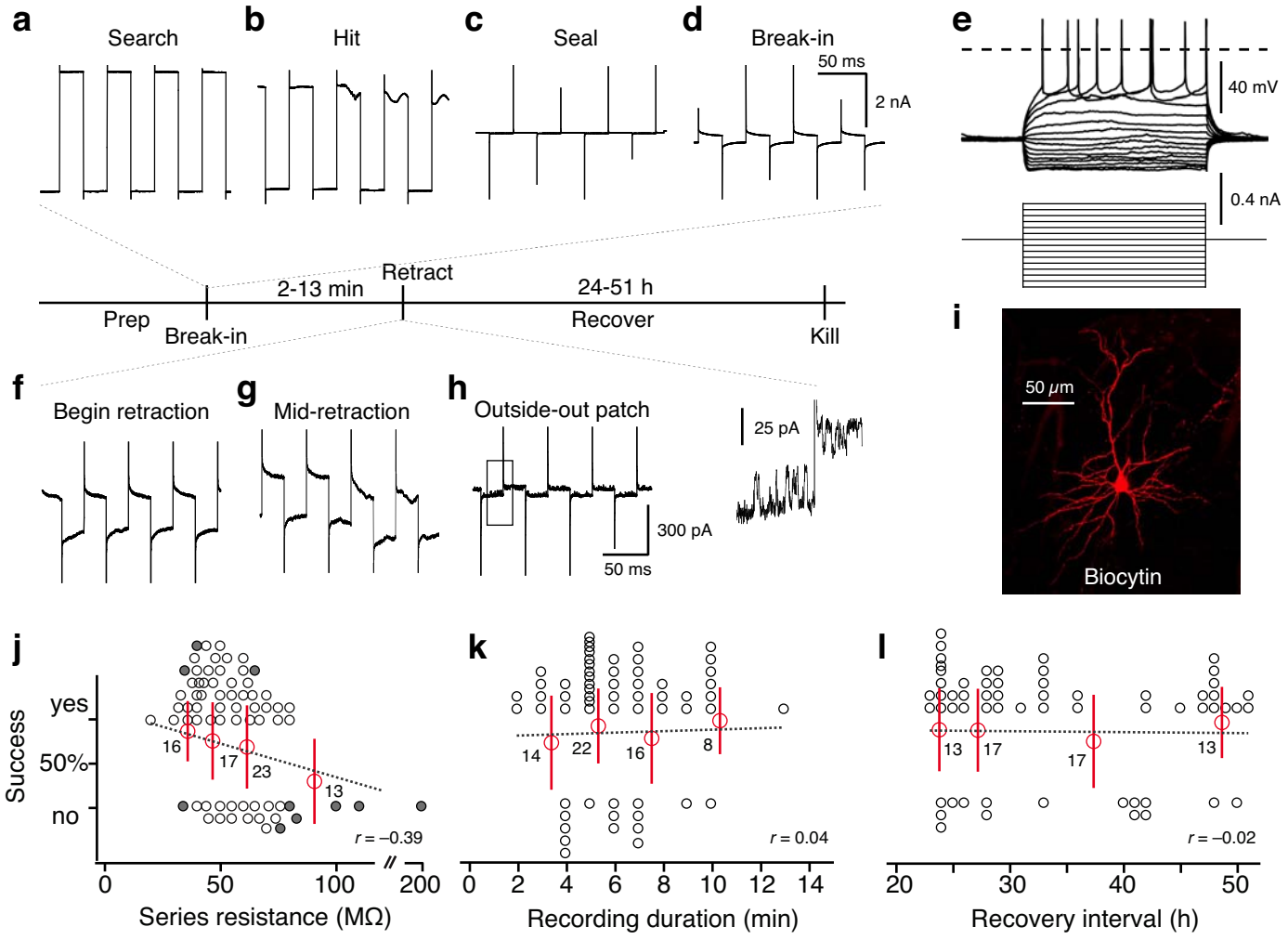

Figure 1 (Rancz etal)

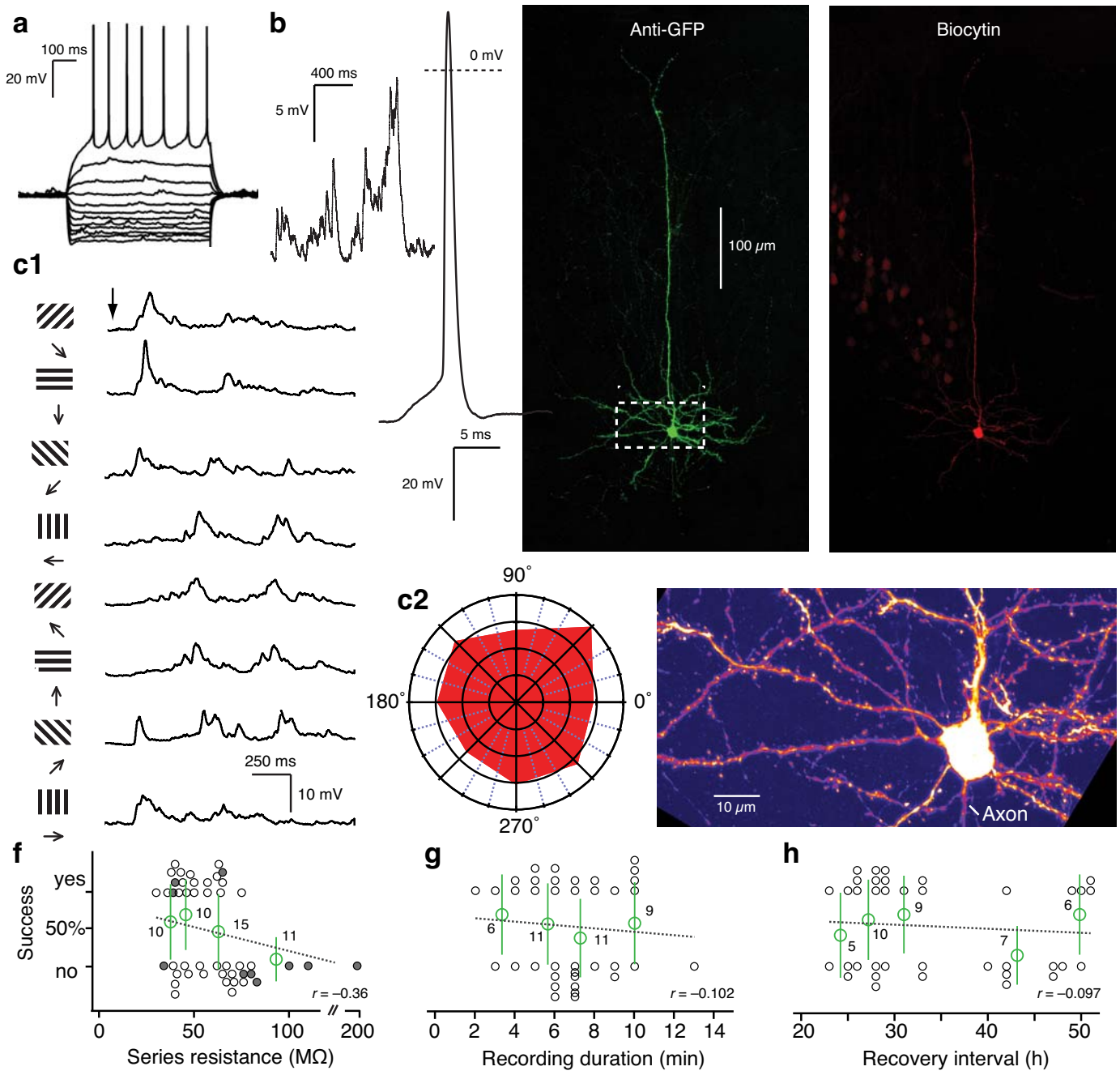

Figure 2 (Rancz etal)

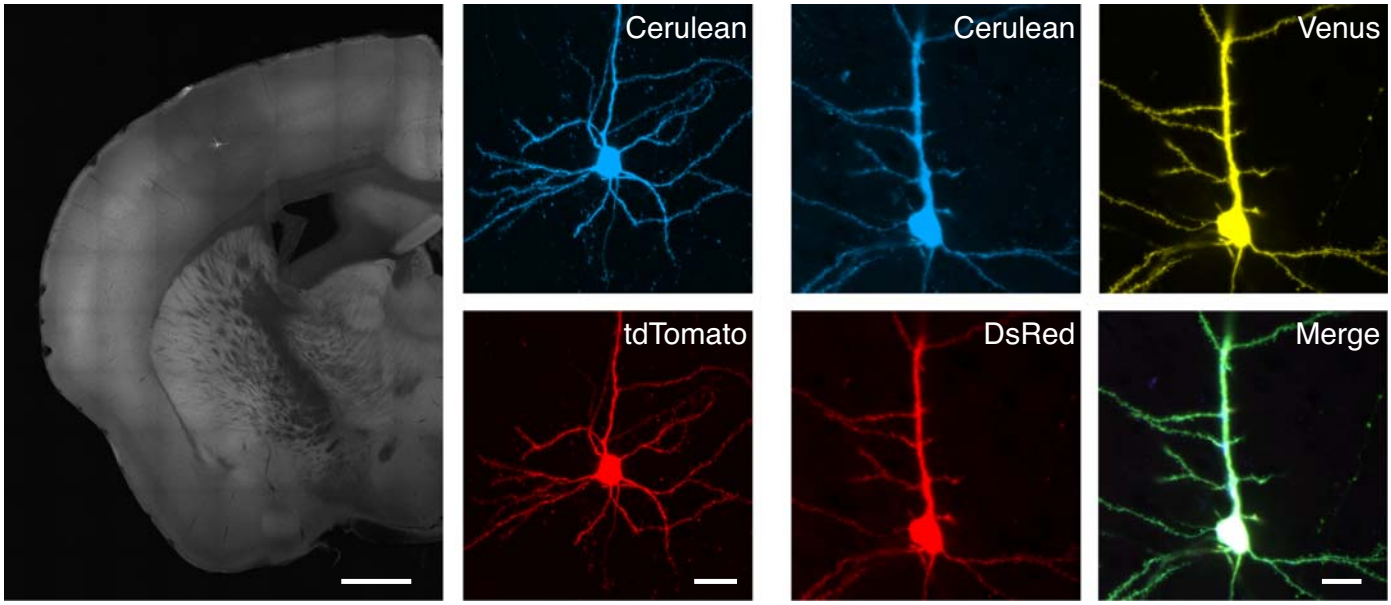

Figure 3 (Rancz etal.)

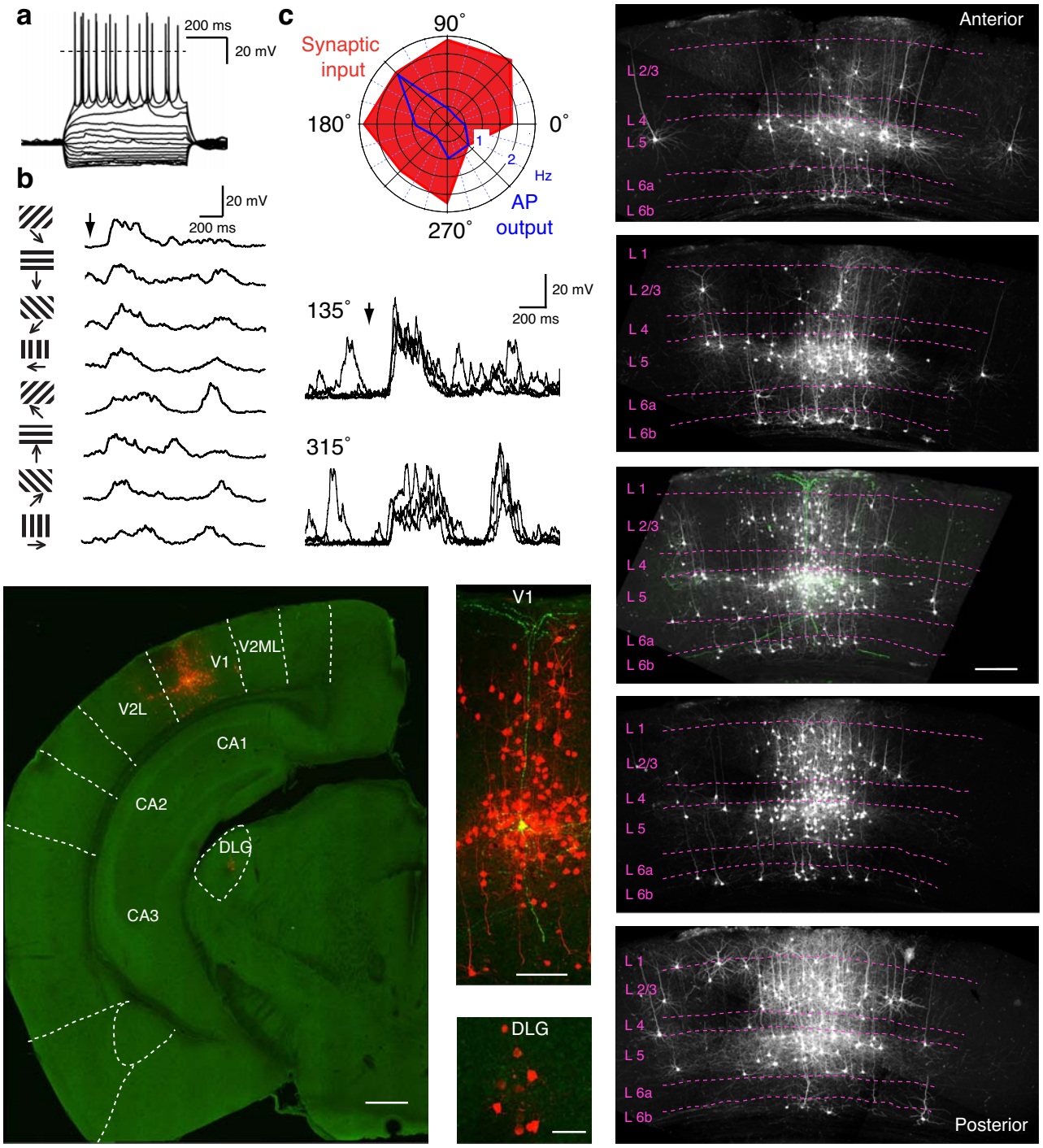

Figure 4 (Rancz etal.)